GEORISK, 2017
VOL. 11, NO. 1, 146–159
http://dx.doi.org/10.1080/17499518.2016.1250279

Taylor & Francis
Taylor & Francis Group

Full probabilistic design of slopes in spatially variable soils using simplified reliability analysis method

Te Xiao, Dian-Qing Li, Zi-Jun Cao and Xiao-Song Tang

State Key Laboratory of Water Resources and Hydropower Engineering Science, Wuhan University, Wuhan, People's Republic of China

ABSTRACT

A simplified reliability analysis method is proposed for efficient full probabilistic design of soil slopes in spatially variable soils. The soil slope is viewed as a series system comprised of numerous potential slip surfaces and the spatial variability of soil properties is modelled by the spatial averaging technique along potential slip surfaces. The proposed approach not only provides sufficiently accurate reliability estimates of slope stability, but also significantly improves the computational efficiency of soil slope design in comparison with simulation-based full probabilistic design. It is found that the spatial variability has considerable effects on the optimal slope design.

ARTICLE HISTORY
Received 29 February 2016
Accepted 16 October 2016

KEYWORDS
Slope; reliability-based design; system reliability analysis; spatial variability; spatial averaging

Notation

FORM	first-order reliability method
MCS	Monte Carlo Simulation
PNET	probabilistic network evaluation technique
QExp	squared exponential (auto-correlation function)
RBD	reliability-based design
RSS	representative slip surface
SExp	single exponential (auto-correlation function)
$P_{f,T}$	target failure probability
$P_{\mathrm{f,sys}}$	system failure probability
n_{SS}	number of potential slip surfaces
n_{RSS}	number of RSSs
$\boldsymbol{R}_{n_{\mathrm{SS}} \times n_{\mathrm{SS}}}$	correlation matrix corresponding to all potential slip surfaces
$\boldsymbol{R}_{n_{\mathrm{RSS}} \times n_{\mathrm{RSS}}}$	correlation matrix corresponding to RSSs
S_p	p-th slip surface
FS_p	factor of safety for S_p
G_p	performance function for S_p
β_p	reliability index for G_p
V_{pk}	segment of S_p in the k-th soil layer
L_{pk}	length of V_{pk}
c	cohesion at the point level
f	friction coefficient at the point level
C_{pk}	spatially averaged cohesion along V_{pk}
F_{pk}	spatially averaged friction coefficient along V_{pk}
γ_{pk}	variance reduction factor of C_{pk} (or F_{pk})
ρ_{pq}	correlation coefficient between G_p and G_q
$\rho_{cf,k}$	cross-correlation coefficient between c and f at the same location of the k-th soil layer
$\rho_{pq,k}$	auto-correlation coefficient between C_{pk} and C_{qk} (or F_{pk} and F_{qk})
ρ_0	correlation coefficient threshold in PNET
X	point uncertain soil property (e.g. c and f)
X_A	spatially averaged uncertain soil property (e.g. C and F)

1. Introduction

In the past few decades, reliability-based design (RBD) has been gaining increasing attentions in geotechnical engineering. For example, the international standard ISO2394:2015 (general principles on reliability of structures) contains an Annex D (reliability of geotechnical structures) that highly advocates the need to develop geotechnical RBD methods (Phoon and Retief 2015). For practical purpose, simplified RBD methods (or semi-probabilistic design methods) are usually adopted in current geotechnical designs, such as load and resistance factor design (e.g. Paikowsky 2004) and multiple resistance factor design (e.g. Phoon, Kulhawy, and Grigoriu 2003) in North America, and Eurocode 7 (e.g. Bond and Harris 2008; Orr 2012) in Europe. These simplified RBD methods have been successfully applied to piles and foundations, but their applications to soil slope designs are rather limited (e.g. Christian 2013; Pantelidis and Griffiths 2014; Salgado and Kim 2014). This

CONTACT Dian-Qing Li dianqing@whu.edu.cn State Key Laboratory of Water Resources and Hydropower Engineering Science, Wuhan University, 8 Donghu South Road, Wuhan 430072, People's Republic of China

can be attributed to, at least partially, two reasons: (1) correlation between load and resistance in slope stability analysis, and (2) existence of numerous correlated failure modes due to the inherent spatial variability of soil properties, which constitute two distinctive elements in RBD of soil slopes.

These two challenges can be easily addressed by full probabilistic design, in which the reliabilities of possible designs are evaluated using reliability analysis methods. Theoretically, all existing reliability analysis methods can be directly used in full probabilistic design with trial-and-error procedure (e.g. Tang, Yucemen, and Ang 1976; Javankhoshdel and Bathurst 2014; Gong et al. 2015; Low and Phoon 2015). In addition to the direct manner, simulation-based reliability analysis methods (e.g. Monte Carlo Simulation (MCS) and Subset Simulation) have been applied to developing more specialised full probabilistic design approaches, such as equivalent design approach (e.g. Ching 2009; Wu et al. 2011) and expanded RBD (e.g. Wang, Au, and Kulhawy 2011; Wang 2013; Wang and Cao 2013; Li et al. 2016a).

Although simulation-based reliability analysis methods are robust and feasible to slope reliability analysis, particularly when spatial variability of soil properties is considered (e.g. Griffiths and Fenton 2004; Wang, Cao, and Au 2011; Kasama and Whittle 2016; Li et al. 2016b, 2016c; Xiao et al. 2016), their computational efforts are generally expensive when they are applied to RBD of soil slopes. Consider a series of possible slope designs. Among these designs, the feasible ones usually have relatively small failure probabilities (i.e. less than target failure probability $P_{f,T}$). To ensure a desired accuracy of reliability estimates, a considerable number of samples are usually needed in simulation-based methods. Moreover, the required number of samples increases with the number of possible designs, leading to a significant increase in computational efforts.

In contrast, simplified reliability analysis methods (e.g. first-order second-moment method and first-order reliability method (FORM)) can evaluate slope reliability efficiently. It is, however, not a trivial task to incorporate spatial variability into slope reliability analysis using simplified reliability analysis methods (e.g. Vanmarcke 1977; Li and Lumb 1987; Christian, Ladd, and Baecher 1994; El-Ramly, Morgenstern, and Cruden 2002; Cho 2007; Ji, Liao, and Low 2012). The complexity in direct spatial variability modelling, such as high-dimensional problem, defeats many existing simplified reliability analysis methods (Schuëller, Pradlwarter, and Koutsourelakis 2004). This issue may be addressed by the spatial averaging technique (e.g. Vanmarcke 2010). Since slope failure is more likely to occur when the average shear strength along a slip surface is insufficient to resist the driving force along the slip surface (El-Ramly, Morgenstern, and Cruden 2002), it is more reasonable to perform spatial averaging along slip surfaces rather than over the whole slope domain (e.g. Suchomel and Mašín 2010). Nevertheless, spatial variability can only be characterised in vertical and horizontal directions due to the testing procedures and limited data in practice (e.g. Fenton 1999; Uzielli, Vannucchi, and Phoon 2005; Cao and Wang 2013, 2014; Lloret-Cabot, Fenton, and Hicks 2014; Wang, Cao, and Li 2016). It is impossible to directly characterise the spatial variability along slip surfaces through site investigation because the actual location of failure slip surface is unknown before slope fails. Furthermore, soil slope may have many potential slip surfaces and shall be viewed as a series system comprised of a number of failure modes (e.g. Oka and Wu 1990; Low, Zhang, and Tang 2011; Zhang, Zhang, and Tang 2011; Cho 2013; Li, Wang, and Cao 2014; Jiang et al. 2015). The spatial variability of soil properties would lessen the correlation among failure modes and strengthen the system effect of slope. How to properly evaluate the correlation among different failure modes with consideration of spatial variability and to incorporate it into slope system reliability analysis using simplified reliability analysis methods remain open questions.

This paper proposes a simplified reliability analysis method for full probabilistic design of slopes in spatially variable soils. The spatial variability of soil properties is explicitly modelled using random field theory, in which spatial averaging is performed along slip surfaces. Correlation among different failure modes is analytically derived accounting for spatial variability and is properly incorporated into slope system reliability analysis. The paper starts with the full probabilistic slope design framework, followed by the development of the simplified reliability analysis method, including system reliability analysis for a given slope design and spatial averaging of soil properties along slip surfaces. Finally, the proposed method is illustrated using two soil slope design examples.

2. Full probabilistic design framework of soil slopes using simplified reliability analysis method

Figure 1 schematically illustrates the full probabilistic soil slope design framework using simplified reliability analysis method. The space of slope design parameters (e.g. slope height and angle) is deliberately discretized into a series of possible designs. For a given design, the simplified reliability analysis method is performed to evaluate the system failure probability $P_{\mathrm{f,sys}}$ of slope stability,

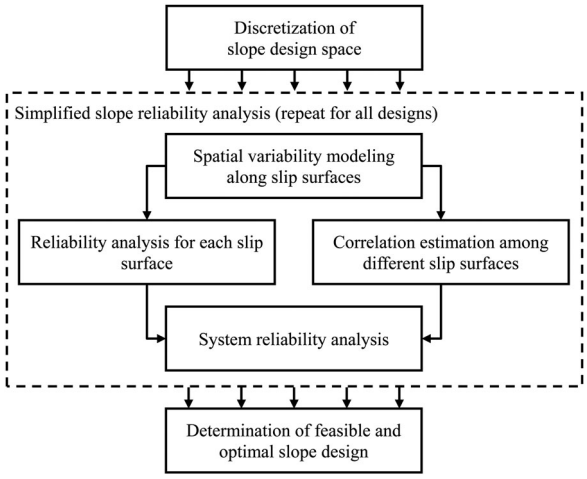

Figure 1. Schematic slope design framework using simplified reliability analysis method.

which is founded on multivariate Gaussian approximation (Hohenbichler and Rackwitz 1982) and the probabilistic network evaluation technique (PNET) (Ang and Tang 1984). There are two major elements in the system reliability analysis, namely, evaluating reliability for each slip surface and estimating correlation among different slip surfaces. The former can be computed using the FORM (Low, Zhang, and Tang 2011; Breitung 2015), and the latter is calculated according to correlations of soil properties. Note that both of them are related to the spatial variability of soil properties. To address the high-dimensional problem in spatial variability modelling, the spatial averaging technique along slip surfaces is adopted based on random field theory (Vanmarcke 2010). After all possible slope designs are assessed, the optimal design is selected from the feasible designs satisfying the reliability requirement (i.e. $P_{\mathrm{f,sys}} \le P_{f,T}$) and with a minimum construction cost (e.g. excavated volume).

Before moving to the development of the proposed approach, two major assumptions on soil properties are given below:

(1) Only spatial variability of shear strength (i.e. cohesion (c) and friction coefficient (f)) and variability of external load are considered. The variability of unit weight is ignored due to its naturally small variability and relatively large spatial averaging area.
(2) Soil properties in different soil layers are assumed independent, while c and f within the same soil layer are assumed to possess the same auto-correlation structure and scale of fluctuation (i.e. consistent spatial variability).

All the discussions in the remaining part of this paper are based on the above two assumptions.

3. System reliability analysis for a given slope design

3.1. System reliability approximation based on representative slip surfaces (RSSs)

Consider, for example, a soil slope with n_{SS} potential slip surfaces, that is, $S_1, S_2, \ldots, S_{n_{\mathrm{SS}}}$, as shown in Figure 2. For a series system, the system failure occurs if any component fails. Hence the system failure probability $P_{\mathrm{f,sys}}$ of slope stability can be written as

$$\begin{aligned} P_{\mathrm{f,sys}} &= P[(G_1 < 0) \cup (G_2 < 0) \cup \ldots \cup (G_{n_{\mathrm{SS}}} < 0)] \\ &= 1 - P[(G_1 \ge 0) \cap (G_2 \ge 0) \cap \ldots \cap (G_{n_{\mathrm{SS}}} \ge 0)], \end{aligned} \tag{1}$$

where G_p, $p = 1, 2, \ldots, n_{\mathrm{SS}}$, is the performance function of S_p. The joint probability in second equality can be evaluated using multivariate Gaussian approximation (or Gaussian Copula) (Hohenbichler and Rackwitz 1982; Tang et al. 2013; Zeng and Jimenez 2014):

$$P_{\mathrm{f,sys}} = 1 - \Phi(\beta_1, \beta_2, \ldots, \beta_{n_{\mathrm{SS}}}; \boldsymbol{R}_{n_{\mathrm{SS}} \times n_{\mathrm{SS}}}), \tag{2}$$

where $\beta_p = \phi^{-1}[P(G_p \ge 0)]$, $p = 1, 2, \ldots, n_{\mathrm{SS}}$, is the reliability index of G_p; $\boldsymbol{R}_{n_{\mathrm{SS}} \times n_{\mathrm{SS}}} = [\rho_{pq}]$ is the correlation matrix corresponding to all potential slip surfaces; ρ_{pq} = correlation coefficient between G_p and G_q; $\phi(\cdot)$ and $\Phi(\cdot)$ are univariate and multivariate standard Gaussian cumulative distribution functions, respectively. However, it is not easy to evaluate high-dimensional multivariate cumulative distribution function, particularly for numerous potential slip surfaces (e.g. $n_{\mathrm{SS}} > 5000$). Moreover, performance functions of some slip surfaces may be highly correlated (i.e. ρ_{pq} is close to unity), resulting in the singularity of $\boldsymbol{R}_{n_{\mathrm{SS}} \times n_{\mathrm{SS}}}$. An example can be found in Low, Zhang, and Tang (2011), as shown in Table 1. As a result, it is impractical to apply Equation (2) to slope system reliability analysis directly.

To address this issue, PNET (Ang and Tang 1984) is adopted to identify a few (e.g. n_{RSS}) relatively independent RSSs of the slope system. In the context of PNET, the slip surface with minimum reliability index is selected as a RSS, and those slip surfaces highly correlated with the RSS (i.e. $\rho_{pq} \ge$ prescribed correlation coefficient threshold ρ_0) are represented by the RSS and

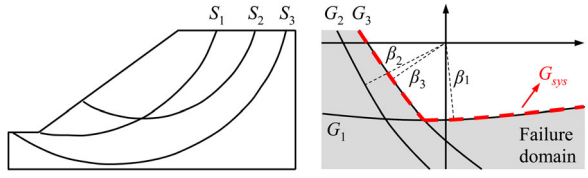

(a) Multiple potential slip surfaces (b) Failure domain in sample space

Figure 2. Illustration of soil slope system.

Table 1. Illustrative example for singular slope system (after Low, Zhang, and Tang (2011)).

Slip surfaces		S_1	S_2	S_3	S_4	S_5	S_6	S_7	S_8
$\boldsymbol{R}_{n_{SS}\times n_{SS}}$	S_1	1	0.454	1	0.456	0.454	1	1	0.531
	S_2		1	0.454	1	1	0.454	0.454	0.996
	S_3			1	0.456	0.454	1	1	0.531
	S_4				1	1	0.456	0.456	0.996
	S_5					1	0.454	0.454	0.996
	S_6						1	1	0.531
	S_7		sys					1	0.531
	S_8								1
β		2.795	2.893	2.837	2.943	2.902	3.047	3.112	3.539

Note: $P_{f,sys}$ cannot be obtained using Equation (2).

excluded from further consideration. This procedure is repeatedly performed for the remaining slip surfaces until all slip surfaces are represented. By this means, the original slope system with n_{SS} potential slip surfaces can be represented by the simplified slope system with n_{RSS} RSSs, and Equation (2) can be approximately estimated as

$$P_{f,sys} \approx 1 - \Phi(\beta_1, \beta_2, \ldots, \beta_{n_{RSS}}; \boldsymbol{R}_{n_{RSS}\times n_{RSS}}), \quad (3)$$

where $\boldsymbol{R}_{n_{RSS}\times n_{RSS}} = [\rho_{pq}]$ is the correlation matrix corresponding to RSSs. Note that all ρ_{pq} values in $\boldsymbol{R}_{n_{RSS}\times n_{RSS}}$ for $p \neq q$ are smaller than ρ_0, which makes $\boldsymbol{R}_{n_{RSS}\times n_{RSS}}$ more likely nonsingular. Applying PNET with $\rho_0 = 0.8$, Table 2 provides a simplified slope system example for that shown in Table 1. Using Equation (3) to evaluate slope system failure probability needs values of β_p and ρ_{pq} ($p = 1, 2, \ldots, n_{SS}$; $q = 1, 2, \ldots, n_{RSS}$), which are calculated in Sections 3.3 and 3.4, respectively. To facilitate understanding, the performance function for a single slip surface is provided in the next subsection prior to calculating β_p and ρ_{pq}.

3.2. Performance function for a single slip surface

In this study, the performance function of slope stability is determined using Ordinary Method of Slices (Duncan and Wright 2014). Based on the total stress analysis method, the factor of safety FS_p of a circular slip surface S_p is calculated as

$$FS_p = \frac{\sum_{i=1}^{n_{sp}} [c_{pi} l_{pi} + f_{pi}(W_{pi} + Q_{pi}) \cos\alpha_{pi}]}{\sum_{i=1}^{n_{sp}} (W_{pi} + Q_{pi}) \sin\alpha_{pi}}, \quad (4)$$

where n_{sp} = number of slices shown in Figure 3(a); c_{pi} and $f_{pi} = \tan\phi_{pi}$ are cohesion and friction coefficient along the base of the i-th slice, respectively; W_{pi} = weight of the i-th slice; $Q_{pi} = qb_{pi}$ is external load acting on top of the i-th slice; q = unit load; b_{pi} = width of the i-th slice; l_{pi} = length of the i-th slice along slip surface; α_{pi} = angle between the base of the i-th slice and the horizontal plane. By setting $FS_p = 1$ as the limit state, the performance function G_p of S_p can be written as

$$G_p = \sum_{i=1}^{n_{sp}} [c_{pi} l_{pi} + f_{pi} W_{pi} \cos\alpha_{pi} + f_{pi} Q_{pi} \cos\alpha_{pi} - W_{pi} \sin\alpha_{pi} - Q_{pi} \sin\alpha_{pi}]. \quad (5)$$

Note that c_{pi} and f_{pi} vary along the slip surface when spatial variability is considered in slope stability analysis (Cho 2007; Ji, Liao, and Low 2012). Hence direct spatial

Table 2. Simplified slope system for illustrative example.

Slip surfaces		S_1	S_2
$\boldsymbol{R}_{n_{RSS}\times n_{RSS}}$	S_1	1	0.454
	S_2	0.454	1
β		2.795	2.893

Note: $P_{f,sys}$ = 0.44% using Equation (3).

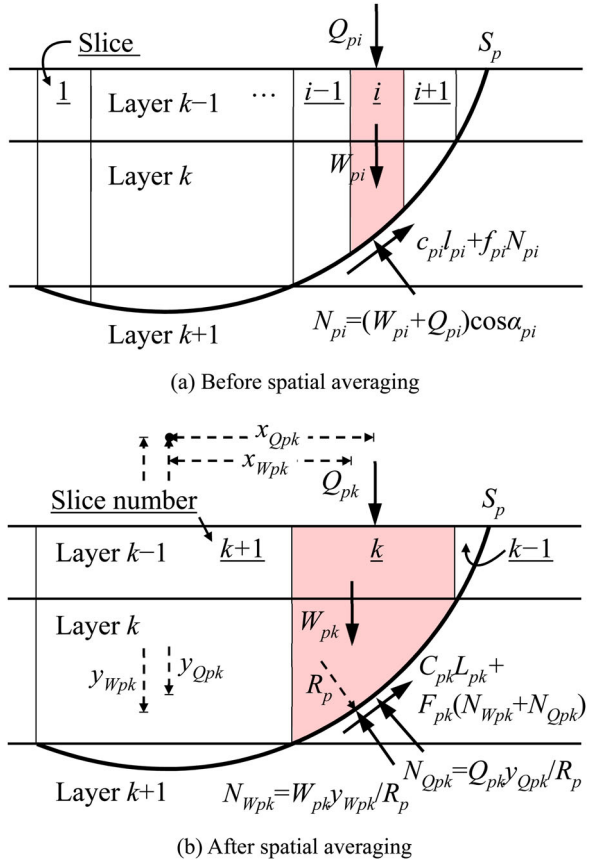

Figure 3. Slope stability analysis using Ordinary Method of Slices.

variability modelling using random field theory will result in high-dimensional difficulty in reliability analysis. To avoid this problem, the spatial averaging technique is adopted in this study. Herein, it is worthwhile to note that the spatial variability of soil properties may lead to non-circular slip surfaces, which can be incorporated in slope reliability analysis using more rigorous probabilistic analysis with direct modelling of spatial variability (Li and Lumb 1987; Griffiths and Fenton 2004; Cho 2007; Ji, Liao, and Low 2012; Tabarroki et al. 2013; Li et al. 2016c). Spatial averaging along non-circular slip surface is more complicated than that along circular slip surface. For simplicity, only circular slip surface is considered in this study. Such a simplification may lead to some errors in estimated slope failure probability due to ignoring non-circular slip surfaces, but this is a good starting point to develop the efficient slope RBD method based on simplified reliability analysis with consideration of spatial variability. Effects of non-circular slip surface on slope failure probability have been explored in literature. Interested readers are referred to Ching, Phoon, and Hu (2010), Tabarroki et al. (2013), and Bahsan et al. (2014).

As shown in Figure 4, each slip surface is partitioned into several segments by soil stratification, for example, segment V_{pk} is a part of S_p located in the k-th soil layer. Likewise, the performance function for a slip surface can be treated as the summation of the performance function for each segment, for example, G_{pk} for V_{pk}. Consider that, for example, resistance from all c_{pi} values along V_{pk} can be written as $\sum(c_{pi}l_{pi}) = C_{pk}\sum l_{pi} = C_{pk}L_{pk}$, in which C_{pk} = spatially averaged cohesion along V_{pk} and $L_{pk} = \sum l_{pi}$ is length of V_{pk}. Analogous spatial averaging is also performed over all f_{pi} values, which leads to F_{pk}, the spatially averaged friction coefficient along V_{pk}. By this means, the original n_{sp} slices are merged into n_{lp} slices corresponding to the soil layer as shown in Figure 3(b), and Equation (5) can be rewritten as

$$G_p = \sum_{k=1}^{n_{lp}} G_{pk} = \sum_{k=1}^{n_{lp}} [C_{pk}L_{pk}R_p + F_{pk}W_{pk}y_{Wpk} + F_{pk}Q_{pk}y_{Qpk} - W_{pk}x_{Wpk} - Q_{pk}x_{Qpk}], \quad (6)$$

where n_{lp} = number of soil layers; $W_{pk} = \sum W_{pi}$ and $Q_{pk} = \sum Q_{pi} = qB_{pk}$ are summations of soil weight and external load acting on V_{pk}, respectively; R_p = radius of S_p; $B_{pk} = \sum b_{pi}$ is width of V_{pk}; $x_{Wpk} = \sum W_{pi}R_p \sin\alpha_{pi}/W_{pk}$, $x_{Qpk} = \sum Q_{pi}R_p \sin\alpha_{pi}/Q_{pk}$, $x_{Qpk} = \sum Q_{pi}R_p \sin\alpha_{pi}/Q_{pk}$ and $y_{Qpk} = \sum Q_{pi}R_p \cos\alpha_{pi}/Q_{pk}$ are horizontal and vertical force moment arms of W_{pk} and Q_{pk} to the centre of slip surface, as shown in Figure 3(b). Since all Q_{pk} values depend on a uniform q, random variables in Equation (6) only contain C_{pk}, F_{pk} ($k = 1, 2, \ldots, n_{lp}$) and q. The spatial averaging technique significantly reduces the number of random variables for G_p from $2n_{sp}+1$ to $2n_{lp}+1$. This lessens the computational difficulty in evaluating β_p and ρ_{pq}.

3.3. Reliability analysis for a single slip surface

Because the performance function defined in Equation (6) is relatively linear, the FORM can be used to evaluate the component reliability index with high accuracy and efficiency, which is written as (Low, Zhang, and Tang 2011; Cho 2013; Breitung 2015; Low and Phoon 2015)

$$\beta_p = \min\{\|\boldsymbol{U}\| | G_p(\boldsymbol{U}) = 0\}, \quad (7)$$

where $\boldsymbol{U}$ = standard normal vector with independent components and it is then converted to original random vector $\boldsymbol{X}_A$ (i.e. the group of C_{pk}, F_{pk} ($k = 1, 2, \ldots, n_{lp}$) and q) by inverse Nataf transformation during the calculation. In the case where point uncertain soil property X (i.e. c or f) is non-normally distributed, the distribution of spatially averaged variable X_A (i.e. C_{pk} or F_{pk}) is technically unknown. Herein, it is assumed that X_A has the same distribution as X. Under this assumption, the whole transformation procedure contains spatial averaging from X to X_A, discussed in Section 4 later, and distribution transformation from X_A to U.

To efficiently evaluate β_p, gradient-based optimisation method (e.g. sequential quadratic programming method) is commonly used in the FORM. For performance function defined in Equation (6), gradients in X_A-space can

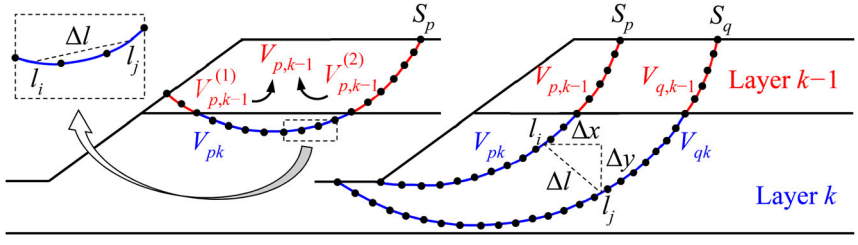

Figure 4. Spatial averaging along slip surfaces.

be analytically calculated as

$$\begin{cases} \dfrac{\partial G_p}{\partial C_{pk}} = L_{pk} R_p, \\ \dfrac{\partial G_p}{\partial F_{pk}} = W_{pk} y_{Wpk} + q B_{pk} y_{Qpk}, \\ \dfrac{\partial G_p}{\partial q} = \displaystyle\sum_{k=1}^{n_{lp}} B_{pk} (F_{pk} y_{Qpk} - x_{Qpk}). \end{cases} \tag{8}$$

They are converted to gradients in U-space according to chain rule of differentiation. Based on Equations (7) and (8), reliability index for each potential slip surface can be obtained efficiently.

3.4. Correlation estimation among different slip surfaces

Consider, for example, performance functions $G_p = \sum_{k=1}^{n_{lp}} G_{pk}$ and $G_q = \sum_{m=1}^{n_{lq}} G_{qm}$ of slip surfaces S_p and S_q, in which G_{pk} and G_{qm} are the performance function of segments V_{pk} and V_{qm}, respectively, and n_{lp} and n_{lq} are the respective number of soil layers that S_p and S_q pass through. Their covariance $Cov(G_p, G_q)$ can be expressed as

$$\begin{aligned} Cov(G_p, G_q) &= Cov\left(\sum_{k=1}^{n_{lp}} G_{pk}, \sum_{m=1}^{n_{lq}} G_{qm} \right) \\ &= \sum_{k=1}^{n_{lp}} \sum_{m=1}^{n_{lq}} Cov(G_{pk}, G_{qm}). \end{aligned} \tag{9}$$

The value of $Cov(G_{pk}, G_{qm})$ is related to the statistics (e.g. standard deviation) of random variables (i.e. C_{pk} and F_{pk} along V_{pk}, C_{qm} and F_{qm} along V_{qm}, and q), auto-correlation coefficient $\rho_{pq,k}$ for C_{pk} and C_{qk} (or F_{pk} and F_{qk}), and cross-correlation coefficient $\rho_{cf,k}$ for c and f in the k-th soil layer. Details of calculating $Cov(G_{pk}, G_{qm})$ can be referred to Appendix A. The variance of G_p can also be calculated through Equation (9) by setting $G_q = G_p$, that is, $Var(G_p) = Cov(G_p, G_p)$. Then, the correlation coefficient ρ_{pq} between G_p and G_q is given by definition,

$$\rho_{pq} = \frac{Cov(G_p, G_q)}{\sqrt{Var(G_p) Var(G_q)}}. \tag{10}$$

Equation (10) gives the element of $\boldsymbol{R}_{n_{SS} \times n_{SS}}$ and $\boldsymbol{R}_{n_{RSS} \times n_{RSS}}$. Based on Equations (9) and (10), the correlation coefficient between two performance functions is analytically calculated from statistics (e.g. standard deviation and correlation coefficient) of spatially averaged variables, which are estimated through the spatial averaging technique in the next section.

4. Spatial averaging of soil properties along slip surfaces

Recall that the slip surface is deliberately partitioned into several segments in different soil layers as shown in Figure 4. Along one of these segments, V_{pk} of S_p for example, the point uncertain soil property X (i.e. c and f) is arithmetically averaged into the spatially averaged variable X_A (i.e. C_{pk} and F_{pk}). According to the random field theory (Vanmarcke 2010), X_A owns a same mean and a reduced variance in comparison with X, that is,

$$\mu_{X_A} = \mu_X, \tag{11}$$

$$\sigma_{X_A} = \sigma_X \sqrt{\gamma_{pk}}, \tag{12}$$

where μ_X and σ_X are mean and standard deviation of X, respectively; μ_{X_A} and σ_{X_A} are mean and standard deviation of X_A, respectively; γ_{pk} = variance reduction factor for X_A along V_{pk} and it is defined as (Vanmarcke 2010)

$$\begin{aligned} \gamma_{pk} &= \frac{1}{L_{pk}^2} \int_0^{L_{pk}} \int_0^{L_{pk}} \rho_1(\Delta l) dl_i dl_j \\ &= \frac{1}{L_{pk}^2} \int_0^{L_{pk}} \int_0^{L_{pk}} \rho_2(\Delta x, \Delta y) dl_i dl_j, \end{aligned} \tag{13}$$

where $\rho_1(\cdot)$ = 1D auto-correlation function along the slip surface with an unknown scale of fluctuation; $\rho_2(\cdot)$ = 2D auto-correlation function with measurable horizontal and vertical scales of fluctuation; Δl, Δx and Δy are, respectively, straight, horizontal and vertical distances between two locations as shown in Figure 4. If a slip surface passes through a soil layer more than once, all parts in the layer shall be integrated into one segment, for example, $V_{p,k-1}^{(1)}$ and $V_{p,k-1}^{(2)}$ are assembled as $V_{p,k-1}$ in Figure 4. The correlation between X_A values along $V_{p,k-1}^{(1)}$ and $V_{p,k-1}^{(2)}$ is also incorporated into the calculation of variance reduction factor. In this way, X_A values of different segments on the same slip surface, for example, $V_{p,k-1}$ and V_{pk}, are independent.

Nevertheless, there exists a correlation among X_A values along segments of different slip surfaces but in the same layer, for example, V_{pk} and V_{qk}. Note that covariance $Cov_{pq,k}$ between C_{pk} and C_{qk} (or F_{pk} and F_{qk}) is defined as (Vanmarcke 2010)

$$Cov_{pq,k} = \frac{1}{L_{pk} L_{qk}} \int_0^{L_{pk}} \int_0^{L_{qk}} Cov_2(\Delta x, \Delta y) dl_i dl_j, \tag{14}$$

where $Cov_2(\cdot)$ = 2D covariance function between two locations. By the definition of covariance, the left-hand and right-hand sides of Equation (14) can be, respectively, written as

$$Cov_{pq,k} = \sigma_{pk} \sigma_{qk} \rho_{pq,k} = \sqrt{\gamma_{pk} \gamma_{qk}} \sigma_X^2 \rho_{pq,k}, \tag{15}$$

$$Cov_2(\Delta x, \Delta y) = \sigma_X^2 \rho_2(\Delta x, \Delta y), \quad (16)$$

where σ_{pk} and σ_{qk} are standard deviations of X_A along V_{pk} and V_{qk}, respectively; $\rho_{pq,k}$ = auto-correlation coefficient between C_{pk} and C_{qk} (or F_{pk} and F_{qk}). Substituting Equations (15) and (16) into Equation (14) gives

$$\rho_{pq,k} = \frac{1}{L_{pk} L_{qk} \sqrt{\gamma_{pk} \gamma_{qk}}} \int_0^{L_{pk}} \int_0^{L_{qk}} \rho_2(\Delta x, \Delta y) dl_i dl_j. \quad (17)$$

Equation (17) describes the auto-correlation between the values of a soil property spatially averaged along different segments in the same layer. It is consistent with Equation (13) when $V_{pk} = V_{qk}$, that is, $\rho_{pq,k} = 1$. In this study, Equations (13) and (17) are integrated numerically according to the slices partitioned in deterministic slope stability analysis, and are rewritten as

$$\gamma_{pk} = \frac{1}{L_{pk}} \sum_{i=1}^{n_{s,pk}} \sum_{j=1}^{n_{s,pk}} \rho_2(\Delta x, \Delta y) l_i l_j, \quad (18)$$

$$\rho_{pq,k} = \frac{1}{L_{pk} L_{qk} \sqrt{\gamma_{pk} \gamma_{qk}}} \sum_{i=1}^{n_{s,pk}} \sum_{j=1}^{n_{s,qk}} \rho_2(\Delta x, \Delta y) l_i l_j, \quad (19)$$

where $n_{s,pk}$ and $n_{s,qk}$ are number of slices contained in V_{pk} and V_{qk}, respectively. Using Equations (18) and (19), variance reduction factors for X_A and auto-correlation coefficients between different X_A values are evaluated, which are utilised to calculate the statistics of X_A in Equations (11) and (12), reliability index of each slip surface in Equation (7), and correlation coefficients between performance functions of different slip surfaces in Equations (9) and (10).

5. Illustrative example I: a two-layered soil slope

For illustration, this section applies the proposed method to RBD of a two-layered soil slope. As shown in Figure 5, the slope has a height H of 5 m and an initial slope angle θ of 26.6° with external load acting on the top of ground surface, which is taken as the nominal design scenario. The statistics of uncertain parameters are summarised in Table 3, all of which are lognormally distributed. Among them, the cohesion and friction coefficient of upper layer soil are considered to be negatively correlated with $\rho_{cf,1} = -0.5$. Furthermore, the spatial variability of soil properties is modelled by single exponential (SExp) auto-correlation function, that is, $\rho_2(\Delta x, \Delta y) = \exp(-2|\Delta x|/\delta_h - 2|\Delta y|/\delta_v)$, with horizontal and vertical scales of fluctuation, δ_h and δ_v, of 20 m and 2 m, respectively.

5.1. System reliability analysis for nominal design scenario

In this subsection, the proposed approach is applied to evaluating the system failure probability $P_{f,sys}$ of the nominal design scenario (i.e. $H = 5$ m, $\theta = 26.6°$). The corresponding results are validated against those obtained from MCS with 100,000 random samples.

For convenience, only three slip surfaces are considered first, as shown in Figure 5. Their corresponding FS values are estimated as 1.484, 1.387 and 2.139, respectively, using Equation (4) based on the mean value of uncertain parameters. The spatial variability of soil properties is modelled through the spatial averaging technique in the simplified reliability analysis method, while it is modelled by direct spatial variability modelling along those slip surfaces in MCS (Cho 2007; Ji, Liao, and Low 2012). Both of them are based on the same discretized locations with horizontal distance smaller than 0.5 m.

In the context of the simplified reliability analysis method, performance functions for all slip surfaces (i.e. Equation (6)) are first determined during the deterministic slope stability analysis. Spatial averaging is then performed, in which variance reduction factors for all the segments (see Table 4 row 2) are calculated using Equation (18) and substituted into Equations (11) and (12) to evaluate the statistics of spatially averaged soil properties. Taking these statistics into the distribution transformation, reliability indices of the three slip surfaces are estimated using Equation (7), and they are 3.394, 2.478 and 11.221, respectively. To enable a fair

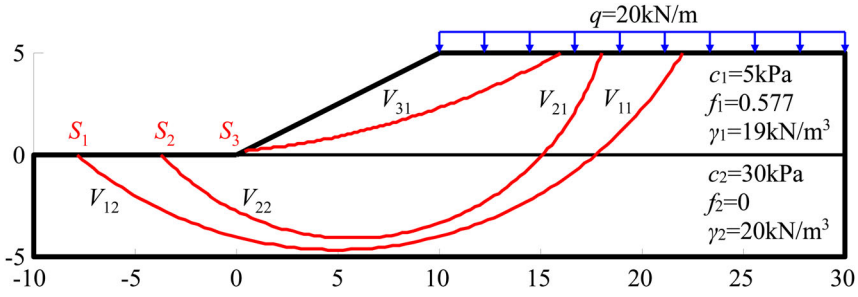

Figure 5. Two-layered soil slope example.

Table 3. Statistics of uncertain parameters for two-layered soil slope example.

Uncertain parameters		Mean	COV	Distribution	Spatial variability	Cross-correlation
Soil layer 1	c_1 (kPa)	5	0.3	Lognormal	SExp [20, 2]	−0.5
	f_1	0.577	0.2	Lognormal	SExp [20, 2]	
Soil layer 2	c_2 (kPa)	30	0.3	Lognormal	SExp [20, 2]	–
q (kN/m)		20	0.1	Lognormal	–	–

Note: SExp [20, 2] = SExp auto-correlation function with $\delta_h = 20$ m and $\delta_v = 2$ m.

comparison with MCS, they are converted to failure probabilities by $P_f = \phi(-\beta)$ (see Table 4 row 5). In addition, correlation coefficients among spatially averaged soil properties along different segments (see Table 4 row 3) are calculated using Equation (19). They are substituted into Equations (9) and (10) to evaluate correlation coefficients among different performance functions for slip surfaces (see Table 4 row 4). Note that correlation coefficients among different performance functions can also be estimated through the FORM by reformulating the performance functions in an enlarged random space. For example, the correlation coefficient between G_1 and G_2 estimated by the FORM in the enlarged variable space is 0.84, which is consistent with that obtained from Equation (10). This verifies the analytical solution derived in this study. Finally, PNET is adopted with $\rho_0 = 0.8$ to identify the RSSs, among which S_2 is the first RSS and S_3 is the second one. The $P_{\text{f,sys}}$ based on S_2 and S_3 is evaluated as 6.6×10^{-3} using Equation (3). In contrast, variance reduction factors and correlation coefficients in MCS are directly estimated through statistical analysis based on the random samples. As shown in Table 4, except the failure probability of S_3, which is too small to be captured by MCS with 100,000 random samples, all the results obtained from the simplified reliability analysis method agree well with those from MCS. This validates the accuracy of the proposed approach.

In order to obtain more accurate $P_{\text{f,sys}}$ of the nominal design scenario, a large amount of potential slip surfaces (about 6000) are considered subsequently, as shown in Figure 6 with grey lines. The minimum FS obtained from deterministic slope stability analysis is 1.371. Since the numbers of slip surfaces and the corresponding discretised locations are large in this case, direct spatial variability modelling for every location along every slip surface (see previous case) is technically formidable for MCS. Instead, the spatial variability is modelled using a random field mesh with an element size of 0.5 m × 0.5 m using the mid-point method (Li et al. 2016b, 2016c). The soil properties within a random field element are assumed to be homogenous, no matter which slip surface passes through the element.

Based on 100,000 random samples, $P_{\text{f,sys}}$ considering all potential slip surfaces is estimated as 3.1% using MCS, which is taken as the "exact" solution as shown in Figure 7(b) with dashed line. In contrast, $P_{\text{f,sys}}$ obtained from the simplified reliability analysis method is evaluated based on RSSs identified by PNET, which relies on the selection of ρ_0. Consider, for example, $\rho_0 = 0.95$. The failure probability of each identified RSS and system failure probability are demonstrated in Figure 7(a) and (b), respectively, by lines with circles. With the maximum RSS number $n_{\max}$ of 25 $P_{\text{f,sys}}$ is estimated as 2.7% using the simplified reliability analysis method, consistent with that (i.e. 3.1%) obtained from MCS. The identified RSSs are plotted in Figure 6 with dark lines, among which the first RSS, also known as probabilistic critical slip surface in literature, is coloured in red. Its failure probability is evaluated as 8.2×10^{-3},

Table 4. Results obtained from simplified reliability analysis method and MCS.

Method		Simplified reliability analysis method			MCS		
Variance reduction for segments		Layer 1		Layer 2	Layer 1		Layer 2
	V_{1k}	0.56		0.46	0.56		0.47
	V_{2k}	0.59		0.50	0.59		0.51
	V_{3k}	0.52		–	0.52		–
Correlation among segments		Layer 1		Layer 2	Layer 1		Layer 2
	V_{1k},V_{2k}	0.71		0.84	0.74		0.84
	V_{1k},V_{3k}	0.38		–	0.36		–
	V_{2k},V_{3k}	0.50		–	0.48		–
Correlation among slip surfaces		S_1	S_2	S_3	S_1	S_2	S_3
	S_1	1	0.84	0.03	1	0.84	0.03
	S_2	0.84	1	0.03	0.84	1	0.03
	S_3	0.03	0.03	1	0.03	0.03	1
Component P_f		S_1	S_2	S_3	S_1	S_2	S_3
		3.4×10^{-4}	6.6×10^{-3}	1.6×10^{-29}	3.2×10^{-4}	6.2×10^{-3}	0
System $P_{f,sys}$			6.6×10^{-3}			6.2×10^{-3}	

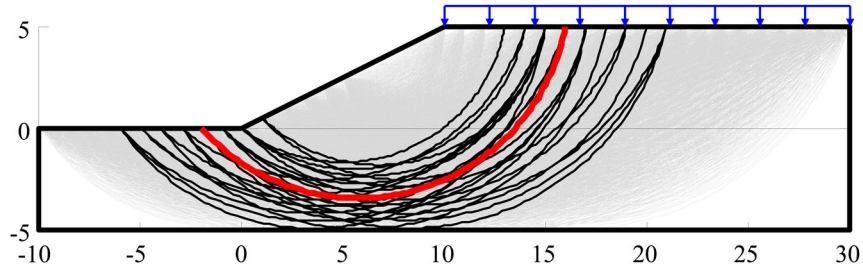

Figure 6. Potential slip surfaces and RSSs identified by PNET ($\rho_0 = 0.95$).

much smaller than the estimated $P_{f,sys}$. Hence only considering the probabilistic critical slip surface in RBD may lead to unconservative slope design, especially for slopes in spatially variable soils. In addition to 0.95, other four ρ_0 values, that is, 0.8, 0.85, 0.9 and 0.99, are also adopted in PNET to determine a proper ρ_0. As illustrated in Figure 7, both the number of RSS and system failure probability increase with increasing ρ_0, indicating that both the computational effort and accuracy for system reliability analysis increase. For slope in spatially variable soils, the spatial variability lessens the correlation among different slip surfaces and strengthens the system effect of slope, thus requiring a relatively high ρ_0 to produce satisfactory results. Trading off accuracy and efficiency, $\rho_0 = 0.95$ with $n_{max} = 25$ appears a prude choice for such a case and it will be applied in the following studies.

With respect to the computational efficiency, the simplified reliability analysis method invokes performance function of each slip surface for nine times on average in this example and takes 1.5 minutes to finish the system reliability analysis on a desktop computer with 8GB RAM and one Intel Corei7 CPU clocked at 3.4 GHz. The MCS, conversely, requires 100,000 calculations for performance function of each slip surface and takes 1.5 hours on the same computer. The high computational efficiency of the proposed approach basically satisfies engineering requirements in practice and can significantly enhance the application of full probabilistic design in soil slopes.

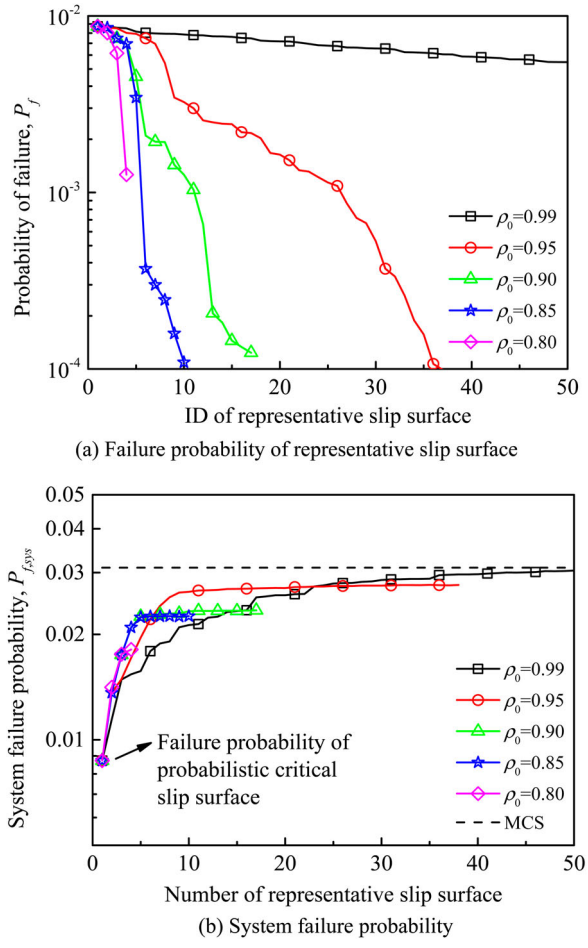

Figure 7. Effect of ρ_0 in system reliability analysis using PNET.

5.2. RBD for the slope

For RBD of the two-layered slope example, two target failure probability levels, that is, $P_{f,T} = 10^{-3}$ and 10^{-4}, are considered in this study. For simplicity, only slope angle θ is taken as the design parameter and the excavated volume of slope is taken as the quantity for measuring construction cost. The design space of θ is discretised into 13 possible designs ranging from 14° to 26° with an increment of 1°. The number of potential slip surface varies from around 4000 to around 6000, due to the variation of ground length for different slope designs with different slope angles. The uncertainties of soil properties are consistent with those in Table 3, and three different external load cases, that is, $\mu_q = 10$, 20 and 30 kN/m with an unchanged $COV_q = 0.1$, are considered to explore the effect of external load on RBD of the slope.

Figure 8 shows the slope failure probabilities and corresponding construction costs for all possible designs using the proposed approach. When $P_{f,T} = 10^{-3}$, the optimal designs for cases with $\mu_q = 10$, 20 and 30 kN/m are 22°, 18° and 15°, respectively. The optimal θ decreases as external load increases. When $P_{f,T}$ decreases to 10^{-4}, the optimal designs for cases with $\mu_q = 10$ and 20 kN/m

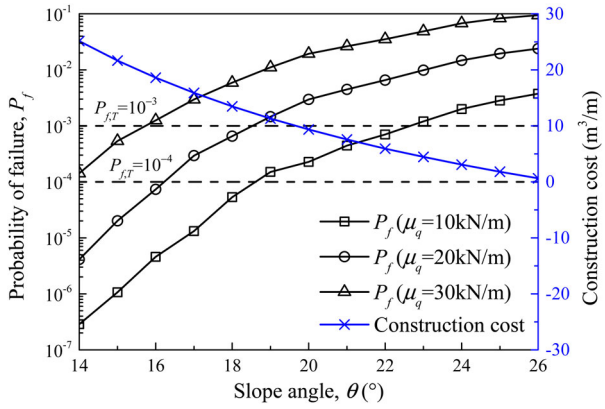

Figure 8. RBD for two-layered soil slope example.

reduce to 18° and 16°, respectively, and no feasible design among the given range can be found for case with μ_q = 30 kN/m. As the reliability requirement increases, the design alteration for the case with smaller external load is more significant than that with larger external load.

5.3. Effect of spatial variability on optimal slope design

A sensitivity study is carried out to explore the effect of spatial variability on RBD of the soil slope, where both influences of auto-correlation function and scale of fluctuation are taken into consideration. Apart from the SExp auto-correlation function, the squared exponential (QExp) auto-correlation function, that is, $\rho_2(\Delta x, \Delta y) = \exp[-\pi(\Delta x/\delta_h)^2 - \pi(\Delta y/\delta_v)^2]$, is also adopted in this subsection. Nine values of δ_h ranging from 10 to 50 m with an increment of 5 m and nine values of δ_v ranging from 2 to 10 m with an increment of 1 m are considered, leading to a total of 81 cases for SExp and QExp auto-correlation functions, respectively. The possible θ values vary from 10° to 26° with an increment of 1° for each case. In addition, the external load μ_q = 10 kN/m and the reliability requirement $P_{f,T} = 10^{-3}$.

Figure 9(a) and (b) demonstrates the design charts for SExp and QExp auto-correlation functions, respectively. Their contours are similar in shape, but quite different in value. The optimal θ based on QExp auto-correlation function is 3°, on average, smaller than that based on SExp auto-correlation function. Using QExp auto-correlation function generates a more conservative design, which was also observed in previous studies (e.g. Li and Lumb 1987; Li et al. 2015). In terms of scale of fluctuation, both horizontal and vertical scales of fluctuation affect optimal design of slope, and the vertical one is more dominative. As scale of fluctuation increases (i.e. spatial correlation increases or spatial variability is less significant), the optimal θ decreases. For the extreme case that soils are

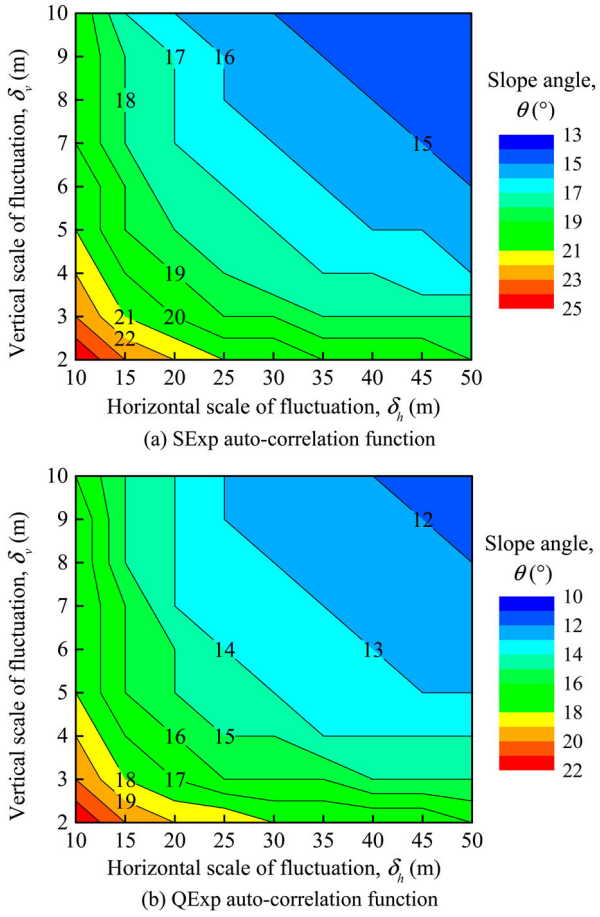

Figure 9. Effect of spatial variability on optimal slope design ($P_{f,T} = 10^{-3}$).

perfectly correlated in space, the optimal θ drops to 10°. Therefore, the spatial variability, including both auto-correlation function and scale of fluctuation, has considerable effects on RBD of soil slopes. Such effects can be properly considered in RBD using the proposed approach.

6. Illustrative example II: a single-layered soil slope

The two-layered slope example shown in Figure 5 is tailored to illustrating the proposed approach in a relatively complicated design situation and has not been used by other investigators. For further validation, this section applies the proposed approach to designing a relatively simple slope shown in Figure 10, which was considered by Wang, Cao, and Au (2011) to explore the effect of spatial variability on system failure probability of slope. As shown in Figure 10, the simple slope example has a height H of 10 m and a slope angle θ of 26.6°, and it has only one single soil layer. The undrained shear strength S_u is modelled by 1D lognormal random field with a mean of 40 kPa, COV of 0.25 and SExp auto-

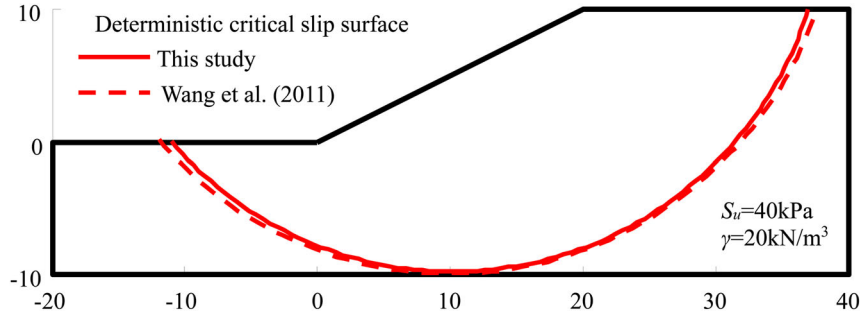

Figure 10. Single-layered soil slope example.

correlation function with $\delta_v = 0.5$ m (Wang, Cao, and Au 2011).

Based on the mean value of S_u, the deterministic critical slip surface (see the solid line in Figure 10) with minimum FS is searched from about 12,000 potential slip surfaces in this study, and the corresponding FS calculated by Equation (4) is 1.180. Both the location and FS of the deterministic critical slip surface agree with those (i.e. the dashed line in Figure 10 and 1.178) reported by Wang, Cao, and Au (2011). Using the proposed approach, the failure probability of deterministic critical slip surface and system failure probability are estimated as 0.16% and 0.89%, respectively, also close to those (i.e. 0.13% and 0.92%) reported by Wang, Cao, and Au (2011) using Subset Simulation. This further validates the proposed approach.

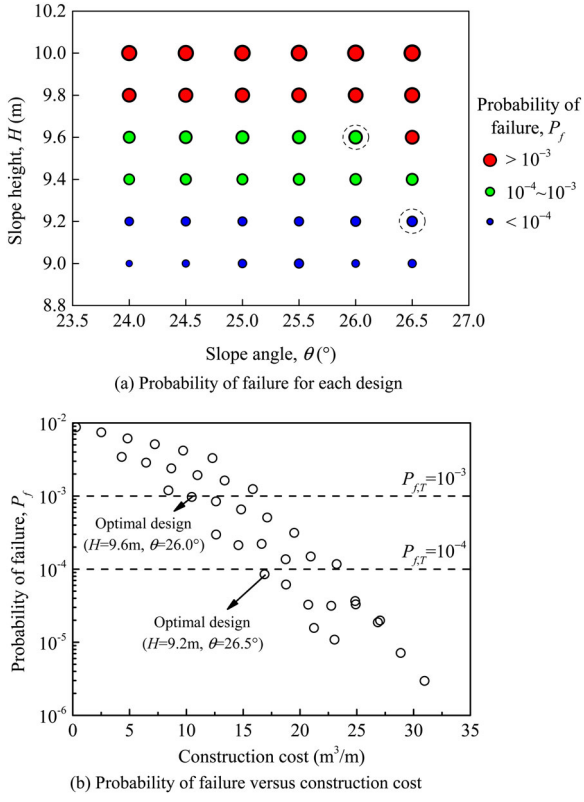

Figure 11. RBD for single-layered soil slope example.

For RBD of the simple slope example, both θ and H are considered as the design parameters and the excavated volume of slope is used again to measure the construction cost. The possible θ values vary from 24.0° to 26.5° with an increment of 0.5° and the possible H values range from 9 to 10 m with an increment of 0.2 m, leading to a total of 36 designs. Figure 11(a) demonstrates the failure probability of each design via a bubble chart, in which larger bubble size means higher failure probability. As shown in Figure 11(a), the failure probability is more sensitive to H than θ in this example. Among the 36 possible designs, 23 designs (i.e. 11 designs in green and 12 designs in blue) are feasible for $P_{f,T} = 10^{-3}$, and 12 designs (i.e. those in blue) are feasible for $P_{f,T} = 10^{-4}$. Further considering the construction cost demonstrated in Figure 11(b), the optimal design is determined as $H = 9.6$ m and $\theta = 26°$ for $P_{f,T} = 10^{-3}$, and $H = 9.2$ m and $\theta = 26.5°$ for $P_{f,T} = 10^{-4}$. They can be obtained using the simplified reliability analysis method with ease.

7. Summary and conclusions

This paper proposed a simplified reliability analysis method for full probabilistic design of slopes in spatially variable soils. For a given design, the spatial variability of soil properties is incorporated into the proposed approach through the spatial averaging technique along potential slip surfaces of the slope system. The statistics of spatially averaged soil properties are then utilised in evaluating the reliability of each slip surface and the correlation among different slip surfaces, in which performance functions for slip surfaces are reformulated to facilitate the spatial averaging. Subsequently, the RSSs are identified from all potential slip surfaces using the probabilistic network evaluation technique. The system failure probability of slope design is finally estimated based on these RSSs by multivariate Gaussian approximation.

Equations were derived for the simplified reliability analysis method and were illustrated by two soil slope

design examples in spatially variable soils. Results were validated against those obtained from MCS. The high computational efficiency provided by the simplified reliability analysis method satisfies engineering requirements in practice and can significantly enhance the application of full probabilistic design in soil slopes. Finally, a sensitivity study was carried out to explore the effects of spatial variability on RBD of soil slopes. It was found that the spatial variability, including both auto-correlation function and scale of fluctuation, has considerable effects on the optimal slope design. Such effects can be properly incorporated into full probabilistic design of soil slopes using the proposed approach.

In the end, it is worthwhile to point out that using Ordinary Method of Slices generally results in conservative designs for circular slip surfaces. The model uncertainty of Ordinary Method of Slices (e.g. Christian, Ladd, and Baecher 1994; Malkawi, Hassan, and Abdulla 2000; Zhang, Zhang, and Tang 2009; Bahsan et al. 2014) may affect the optimal slope design more or less. However, research is rare that calibrated the model uncertainty of Ordinary Method of Slices in multi-layered slope stability analysis considering spatial variability. More efforts on calibrating the model uncertainty in such cases and incorporating it into RBD of soil slopes are still warranted.

Disclosure statement

No potential conflict of interest was reported by the authors.

Funding

This work was supported by the National Science Fund for Distinguished Young Scholars (Project No. 51225903), the National Natural Science Foundation of China (Project Nos. 51329901, 51579190, 51679174), and the Natural Science Foundation of Hubei Province of China (Project No. 2014CFA001). The financial support is gratefully acknowledged.

References

Ang, A. H.-S., and W. H. Tang. 1984. *Probability Concepts in Engineering Planning and Design, Vol. 2: Design, Risk, and Reliability*. New York: John Wiley & Sons.

Bahsan, E., H. J. Liao, J. Ching, and S. W. Lee. 2014. "Statistics for the Calculated Safety Factors of Undrained Failure Slopes." *Engineering Geology* 172: 85–94.

Bond, A., and A. Harris. 2008. *Decoding Eurocode 7*. London: Taylor & Francis.

Breitung, K. 2015. "40 Years FORM: Some New Aspects?" *Probabilistic Engineering Mechanics* 42: 71–77.

Cao, Z., and Y. Wang. 2013. "Bayesian Approach for Probabilistic Site Characterization Using Cone Penetration Tests." *Journal of Geotechnical and Geoenvironmental Engineering* 139 (2): 267–276.

Cao, Z., and Y. Wang. 2014. "Bayesian Model Comparison and Selection of Spatial Correlation Functions for Soil Parameters." *Structural Safety* 49: 10–17.

Ching, J. 2009. "Equivalence Between Reliability and Factor of Safety." *Probabilistic Engineering Mechanics* 24 (2): 159–171.

Christian, J. T. 2013. "Issues of Reliability in Stability of Slopes." In Proceedings of Geo-Congress 2013: Stability and Performance of Slopes and Embankments III, San Diego, California, United States, March 3–7 2013, 2246–2261.

Ching, J., K. K. Phoon, and Y. G. Hu. 2010. "Observations on Limit Equilibrium-Based Slope Reliability Problems with Inclined Weak Seams." *Journal of Engineering Mechanics* 136 (10): 1220–1233.

Christian, J. T., C. C. Ladd, and G. B. Baecher. 1994. "Reliability Applied to Slope Stability Analysis." *Journal of Geotechnical Engineering* 120 (12): 2180–2207.

Cho, S. E. 2007. "Effects of Spatial Variability of Soil Properties on Slope Stability." *Engineering Geology* 92 (3): 97–109.

Cho, S. E. 2013. "First-order Reliability Analysis of Slope Considering Multiple Failure Modes." *Engineering Geology* 154: 98–105.

Duncan, J. M., and S. G. Wright. 2014. *Soil Strength and Slope Stability*. 2nd ed. Hoboken, NJ: John Wiley & Sons.

El-Ramly, H., N. R. Morgenstern, and D. M. Cruden. 2002. "Probabilistic Slope Stability Analysis for Practice." *Canadian Geotechnical Journal* 39 (3): 665–683.

Fenton, G. A. 1999. "Estimation for Stochastic Soil Models." *Journal of Geotechnical and Geoenvironmental Engineering* 125 (6): 470–485.

Gong, W., L. Wang, S. Khoshnevisan, C. H. Juang, H. Huang, and J. Zhang. 2015. "Robust Geotechnical Design of Earth Slopes Using Fuzzy Sets." *Journal of Geotechnical and Geoenvironmental Engineering* 141 (1): 04014084.

Griffiths, D. V., and G. A. Fenton. 2004. "Probabilistic Slope Stability Analysis by Finite Elements." *Journal of Geotechnical and Geoenvironmental Engineering* 130 (5): 507–518.

Hohenbichler, M., and R. Rackwitz. 1982. "First-order Concepts in System Reliability." *Structural Safety* 1 (3): 177–188.

Javankhoshdel, S., and R. J. Bathurst. 2014. "Simplified Probabilistic Slope Stability Design Charts for Cohesive and Cohesive-Frictional (c-φ) Soils." *Canadian Geotechnical Journal* 51 (9): 1033–1045.

Ji, J., H. J. Liao, and B. K. Low. 2012. "Modeling 2-D Spatial Variation in Slope Reliability Analysis Using Interpolated Autocorrelations." *Computers and Geotechnics* 40: 135–146.

Jiang, S. H., D. Q. Li, Z. J. Cao, C. B. Zhou, and K. K. Phoon. 2015. "Efficient System Reliability Analysis of Slope Stability in Spatially Variable Soils Using Monte Carlo Simulation." *Journal of Geotechnical and Geoenvironmental Engineering* 141 (2): 04014096.

Kasama, K., and A. J. Whittle. 2016. "Effect of Spatial Variability on the Slope Stability Using Random Field Numerical Limit Analyses." *Georisk: Assessment and Management of Risk for Engineered Systems and Geohazards* 10 (1): 42–54.

Li, D. Q., S. H. Jiang, Z. J. Cao, W. Zhou, C. B. Zhou, and L. M. Zhang. 2015. "A Multiple Response-Surface Method for Slope Reliability Analysis Considering Spatial Variability of Soil Properties." *Engineering Geology* 187: 60–72.

Li, K. S., and P. Lumb. 1987. "Probabilistic Design of Slopes." *Canadian Geotechnical Journal* 24 (4): 520–535.
Li, D. Q., K. B. Shao, Z. J. Cao, X. S. Tang, and K. K. Phoon. 2016a. "A Generalized Surrogate Response Aided-Subset Simulation Approach for Efficient Geotechnical Reliability-Based Design." *Computers and Geotechnics* 74: 88–101.
Li, L., Y. Wang, and Z. Cao. 2014. "Probabilistic Slope Stability Analysis by Risk Aggregation." *Engineering Geology* 176: 57–65.
Li, D. Q., T. Xiao, Z. J. Cao, K. K. Phoon, and C. B. Zhou. 2016b. "Efficient and Consistent Reliability Analysis of Soil Slope Stability Using Both Limit Equilibrium Analysis and Finite Element Analysis." *Applied Mathematical Modelling* 40 (9–10): 5216–5229.
Li, D. Q., T. Xiao, Z. J. Cao, C. B. Zhou, and L. M. Zhang. 2016c. "Enhancement of Random Finite Element Method in Reliability Analysis and Risk Assessment of Soil Slopes Using Subset Simulation." *Landslides* 13: 293–303.
Lloret-Cabot, M., G. A. Fenton, and M. A. Hicks. 2014. "On the Estimation of Scale of Fluctuation in Geostatistics." *Georisk: Assessment and Management of Risk for Engineered Systems and Geohazards* 8 (2): 129–140.
Low, B. K., and K. K. Phoon. 2015. "Reliability-based Design and Its Complementary Role to Eurocode 7 Design Approach." *Computers and Geotechnics* 65: 30–44.
Low, B. K., J. Zhang, and W. H. Tang. 2011. "Efficient System Reliability Analysis Illustrated for a Retaining Wall and a Soil Slope." *Computers and Geotechnics* 38 (2): 196–204.
Malkawi, A. I. H., W. F. Hassan, and F. A. Abdulla. 2000. "Uncertainty and Reliability Analysis Applied to Slope Stability." *Structural Safety* 22 (2): 161–187.
Oka, Y., and T. H. Wu. 1990. "System Reliability of Slope Stability." *Journal of Geotechnical Engineering* 116 (8): 1185–1189.
Orr, T. L. L. 2012. "How Eurocode 7 Has Affected Geotechnical Design: A Review." *Proceedings of the Institution of Civil Engineers - Geotechnical Engineering* 165 (6): 337–350.
Paikowsky, S. G. 2004. *Load and Resistance Factor Design (LRFD) for Deep Foundations*. NCHRP Report 507. Washington, DC: Transportation Research Board.
Pantelidis, L., and D. V. Griffiths. 2014. "Integrating Eurocode 7 (Load and Resistance Factor Design) Using Nonconventional Factoring Strategies in Slope Stability Analysis." *Canadian Geotechnical Journal* 51 (2): 208–216.
Phoon, K. K., F. H. Kulhawy, and M. D. Grigoriu. 2003. "Multiple Resistance Factor Design for Shallow Transmission Line Structure Foundations." *Journal of Geotechnical and Geoenvironmental Engineering* 129 (9): 807–818.
Phoon, K. K., and J. V. Retief. 2015. "ISO2394: 2015 Annex D (Reliability of Geotechnical Structures)." *Georisk: Assessment and Management of Risk for Engineered Systems and Geohazards* 9 (3): 125–127.
Salgado, R., and D. Kim. 2014. "Reliability Analysis of Load and Resistance Factor Design of Slopes." *Journal of Geotechnical and Geoenvironmental Engineering* 140 (1): 57–73.
Schuëller, G. I., H. J. Pradlwarter, and P. S. Koutsourelakis. 2004. "A Critical Appraisal of Reliability Estimation Procedures for High Dimensions." *Probabilistic Engineering Mechanics* 19 (4): 463–474.
Suchomel, R., and D. Mašín. 2010. "Comparison of Different Probabilistic Methods for Predicting Stability of A Slope in Spatially Variable c–ϕ Soil." *Computers and Geotechnics* 37 (1): 132–140.
Tabarroki, M., F. Ahmad, R. Banaki, S. K. Jha, and J. Ching. 2013. "Determining the Factors of Safety of Spatially Variable Slopes Modeled by Random Fields." *Journal of Geotechnical and Geoenvironmental Engineering* 139 (12): 2082–2095.
Tang, X. S., D. Q. Li, C. B. Zhou, K. K. Phoon, and L. M. Zhang. 2013. "Impact of Copulas for Modeling Bivariate Distributions on System Reliability." *Structural Safety* 44: 80–90.
Tang, W. H., M. S. Yucemen, and A. H.-S. Ang. 1976. "Probability-based Short Term Design of Soil Slopes." *Canadian Geotechnical Journal* 13 (3): 201–215.
Uzielli, M., G. Vannucchi, and K. K. Phoon. 2005. "Random Field Characterisation of Stress-Nomalised Cone Penetration Testing Parameters." *Geotechnique* 55 (1): 3–20.
Vanmarcke, E. H. 1977. "Reliability of Earth Slopes." *Journal of the Geotechnical Engineering Division* 103 (11): 1247–1265.
Vanmarcke, E. H. 2010. *Random Fields: Analysis and Synthesis (Revised and Expanded new Edition)*. Singapore: World Scientific Publishing.
Vořechovský, M. 2008. "Simulation of Simply Cross Correlated Random Fields by Series Expansion Methods." *Structural Safety* 30 (4): 337–363.
Wang, Y. 2013. "MCS-based Probabilistic Design of Embedded Sheet Pile Walls." *Georisk: Assessment and Management of Risk for Engineered Systems and Geohazards* 7 (3): 151–162.
Wang, Y., S. K. Au, and F. H. Kulhawy. 2011. "Expanded Reliability-based Design Approach for Drilled Shafts." *Journal of Geotechnical and Geoenvironmental Engineering* 137 (2): 140–149.
Wang, Y., and Z. Cao. 2013. "Expanded Reliability-Based Design of Piles in Spatially Variable Soil Using Efficient Monte Carlo Simulations." *Soils and Foundations* 53 (6): 820–834.
Wang, Y., Z. Cao, and S. K. Au. 2011. "Practical Reliability Analysis of Slope Stability by Advanced Monte Carlo Simulations in a Spreadsheet." *Canadian Geotechnical Journal* 48 (1): 162–172.
Wang, Y., Z. Cao, and D. Li. 2016. "Bayesian Perspective on Geotechnical Variability and Site Characterization." *Engineering Geology* 203: 117–125.
Wu, S. H., C. Y. Ou, J. Ching, and C. H. Juang. 2011. "Reliability-based Design for Basal Heave Stability of Deep Excavations in Spatially Varying Soils." *Journal of Geotechnical and Geoenvironmental Engineering* 138 (5): 594–603.
Xiao, T., D. Q. Li, Z. J. Cao, S. K. Au, and K. K. Phoon. 2016. "Three-dimensional Slope Reliability and Risk Assessment Using Auxiliary Random Finite Element Method." *Computers and Geotechnics* 79: 146–158.
Zeng, P., and R. Jimenez. 2014. "An Approximation to the Reliability of Series Geotechnical Systems Using A Linearization Approach." *Computers and Geotechnics* 62: 304–309.
Zhang, J., L. M. Zhang, and W. H. Tang. 2009. "Bayesian Framework for Characterizing Geotechnical Model Uncertainty." *Journal of Geotechnical and Geoenvironmental Engineering* 135 (7): 932–940.
Zhang, J., L. M. Zhang, and W. H. Tang. 2011. "New Methods for System Reliability Analysis of Soil Slopes." *Canadian Geotechnical Journal* 48 (7): 1138–1148.

Appendix A. Covariance between two performance functions

For simplicity, performance functions G_{pk} and G_{qm} (see Equation (6)) corresponding to segments V_{pk} and V_{qm} are rewritten as

$$\begin{aligned} G_{pk} &= k_{0pk} + k_{1pk}X_{1pk} + k_{2pk}X_{2pk} + k_{3pk}X_{3pk} + k_{4pk}X_{2pk}X_{3pk} \\ G_{qm} &= k_{0qm} + k_{1qm}X_{1qm} + k_{2qm}X_{2qm} + k_{3qm}X_{3qm} + k_{4qm}X_{2qm}X_{3qm}, \end{aligned} \tag{A1}$$

where $k_{0s} = -W_s x_{Ws}$, $k_{1s} = L_s R_s$, $k_{2s} = W_s y_{Ws}$, $k_{3s} = -x_{Qs}$, $k_{4s} = y_{Qs}$, $X_{1s} = C_s$, $X_{2s} = F_s$ and $X_{3s} = Q_s$ ($s = pk$, qm).

The correlation between G_{pk} and G_{qm} comes from two parts, including auto-correlation for the same soil property and cross-correlation for different soil properties. The auto-correlation (see Section 4) for X_{1pk} and X_{1qm} (C), X_{2pk} and X_{2qm} (F) and X_{3pk} and X_{3qm} (Q) are $\rho_{pq,km}$, $\rho_{pq,km}$ and 1, respectively, where $\rho_{pq,km} = \rho_{pq,k}$ for $k = m$ and $\rho_{pq,km} = 0$ for $k \neq m$; $\rho_{pq,k}$ = auto-correlation coefficient between C_{pk} and C_{qk} (or F_{pk} and F_{qk}) spatially averaged along V_{pk} and V_{qk} in the k-th soil layer, which can be calculated by Equation (19). The cross-correlation between c and f for different locations, denoted as a and b, within the k-th soil layer follows the assumption that $\rho(c_{ak}, f_{bk}) = \rho_{cf,k} \times \rho_{ab}$, where $\rho_{cf,k}$ = cross-correlation coefficient between c and f at the same location of the k-th soil layer; ρ_{ab} = auto-correlation coefficient for same soil property between locations a and b. This assumption is consistent with previous studies (Vořechovský 2008; Ji, Liao, and Low 2012) and can be extended to spatially averaged soil properties, that is, $\rho(C_{pk}, F_{qm}) = \rho_{cf,km} \times \rho_{pq,km}$, where $\rho_{cf,km} = \rho_{cf,k}$ for $k = m$ and $\rho_{cf,km} = 0$ for $k \neq m$.

Based on the abovementioned relationship, $Cov(G_{pk}, G_{qm})$ can be calculated as

$$\begin{aligned} Cov(G_{pk}, G_{qm}) &= [Cov(G_{pk}, G_{qm})]_A + [Cov(G_{pk}, G_{qm})]_C \\ &= \begin{bmatrix} k_{1pk}k_{1qm}Cov(X_{1pk}, X_{1qm}) + k_{2pk}k_{2qm}Cov(X_{2pk}, X_{2qm}) + \\ k_{3pk}k_{3qm}Cov(X_{3pk}, X_{3qm}) + k_{4pk}k_{4qm}Cov(X_{2pk}X_{3pk}, X_{2qm}X_{3qm}) + \\ k_{2pk}k_{4qm}Cov(X_{2pk}, X_{2qm}X_{3qm}) + k_{2qm}k_{4pk}Cov(X_{2qm}, X_{2pk}X_{3pk}) + \\ k_{3pk}k_{4qm}Cov(X_{3pk}, X_{2qm}X_{3qm}) + k_{3qm}k_{4pk}Cov(X_{3qm}, X_{2pk}X_{3pk}) \end{bmatrix}_A \\ &+ \begin{bmatrix} k_{1pk}k_{2qm}Cov(X_{1pk}, X_{2qm}) + k_{1qm}k_{2pk}Cov(X_{1qm}, X_{2pk}) + \\ k_{1pk}k_{4qm}Cov(X_{1pk}, X_{2qm}X_{3qm}) + k_{1qm}k_{4pk}Cov(X_{1qm}, X_{2pk}X_{3pk}) \end{bmatrix}_C \\ &= \begin{bmatrix} k_{1pk}k_{1qm}\rho_{pq,km}\tilde{X}_{1pk}\tilde{X}_{1qm} + k_{2pk}k_{2qm}\rho_{pq,km}\tilde{X}_{2pk}\tilde{X}_{2qm} + k_{3pk}k_{3qm}\tilde{X}_{3pk}\tilde{X}_{3qm} + \\ k_{4pk}k_{4qm}(\bar{X}_{2pk}\bar{X}_{2qm}\tilde{X}_{3pk}\tilde{X}_{3qm} + \rho_{pq,km}\tilde{X}_{2pk}\tilde{X}_{2qm}\bar{X}_{3pk}\bar{X}_{3qm} + \rho_{pq,km}\tilde{X}_{2pk}\tilde{X}_{2qm}\tilde{X}_{3pk}\tilde{X}_{3qm}) + \\ k_{2pk}k_{4qm}\rho_{pq,km}\tilde{X}_{2pk}\tilde{X}_{2qm}\bar{X}_{3qm} + k_{2qm}k_{4pk}\rho_{pq,km}\tilde{X}_{2qm}\tilde{X}_{2pk}\bar{X}_{3pk} + \\ k_{3pk}k_{4qm}\tilde{X}_{3pk}\tilde{X}_{3qm}\bar{X}_{2qm} + k_{3qm}k_{4pk}\tilde{X}_{3qm}\tilde{X}_{3pk}\bar{X}_{2pk} \end{bmatrix}_A \\ &+ \begin{bmatrix} k_{1pk}k_{2qm}\rho_{cf,km}\rho_{pq,km}\tilde{X}_{1pk}\tilde{X}_{2qm} + k_{1qm}k_{2pk}\rho_{cf,km}\rho_{pq,km}\tilde{X}_{1qm}\tilde{X}_{2pk} + \\ k_{1pk}k_{4qm}\rho_{cf,km}\rho_{pq,km}\tilde{X}_{1pk}\tilde{X}_{2qm}\bar{X}_{3qm} + k_{1qm}k_{4pk}\rho_{cf,km}\rho_{pq,km}\tilde{X}_{1qm}\tilde{X}_{2pk}\bar{X}_{3pk} \end{bmatrix}_C \end{aligned} \tag{A2}$$

where subscripts "A" and "C" denote auto-correlation and cross-correlation, respectively; hats "$-$" and "$\sim$" denote mean and standard deviation, respectively. In Equation (A2), the covariance items can be derived from the definition of covariance and the equality that $Cov(Y, Z) = E(YZ) - E(Y)E(Z)$, where $E(\cdot)$ = expectation operation. For instance,

$$\begin{aligned} &Cov(X_{2pk}X_{3pk}, X_{2qm}X_{3qm}) = E(X_{2pk}X_{3pk}X_{2qm}X_{3qm}) - E(X_{2pk}X_{3pk})E(X_{2qm}X_{3qm}) \\ &= E(X_{2pk}X_{2qm})E(X_{3pk}X_{3qm}) - \bar{X}_{2pk}\bar{X}_{3pk}\bar{X}_{2qm}\bar{X}_{3qm} \\ &= [\bar{X}_{2pk}\bar{X}_{2qm} + Cov(X_{2pk}, X_{2qm})][\bar{X}_{3pk}\bar{X}_{3qm} + Cov(X_{3pk}, X_{3qm})] - \bar{X}_{2pk}\bar{X}_{3pk}\bar{X}_{2qm}\bar{X}_{3qm} \\ &= \bar{X}_{2pk}\bar{X}_{2qm}Cov(X_{3pk}, X_{3qm}) + \bar{X}_{3pk}\bar{X}_{3qm}Cov(X_{2pk}, X_{2qm}) + Cov(X_{2pk}, X_{2qm})Cov(X_{3pk}, X_{3qm}) \\ &= \bar{X}_{2pk}\bar{X}_{2qm}\tilde{X}_{3pk}\tilde{X}_{3qm} + \rho_{pq,km}\tilde{X}_{2pk}\tilde{X}_{2qm}\bar{X}_{3pk}\bar{X}_{3qm} + \rho_{pq,km}\tilde{X}_{2pk}\tilde{X}_{2qm}\tilde{X}_{3pk}\tilde{X}_{3qm} \end{aligned} \tag{A3}$$

Similarly,

$$Cov(X_{2pk}, X_{2qm}X_{3qm}) = \bar{X}_{3qm}Cov(X_{2pk}, X_{2qm}) = \rho_{pq,km}\tilde{X}_{2pk}\tilde{X}_{2qm}\bar{X}_{3qm}. \tag{A4}$$

The other covariance items can be derived in a similar way. Although Equation (A2) appears complicated, the calculation can be finished with relative ease since it is an explicit function of the statistics for uncertain parameters and those statistics have been determined before reliability analysis.